OXFORD JLB JOURNAL OF LEUKOCYTE BIOLOGY

Journal of Leukocyte Biology, 2024, **115**, 222–234

https://doi.org/10.1093/jleuko/qiad137
Advance access publication 7 November 2023
Review Article

Panton-Valentine leukocidin–induced neutrophil extracellular traps lack antimicrobial activity and are readily induced in patients with recurrent PVL $^{+}$ - *Staphylococcus aureus* infections

Hina Jhelum,[1,†] Dora Čerina,[1,†] C.J. Harbort,[1] Andreas Lindner,[2] Leif Gunnar Hanitsch,[3] Rasmus Leistner,[4] Jennyver-Tabea Schröder,[5] Horst von Bernuth,[6,7,8,9] Miriam Songa Stegemann,[10] Mariana Schürmann,[10] Arturo Zychlinsky,[1] Renate Krüger,[6,‡] and Gerben Marsman[1,*,‡]

[1]Department of Cellular Microbiology, Max Planck Institute for Infection Biology, Charitéplatz 1, 10117, Berlin, Germany
[2]Institute of Tropical Medicine and International Health, Charité—Universitätsmedizin Berlin, corporate member of Freie Universität Berlin, Humboldt-Universität zu Berlin, and Berlin Institute of Health, Charitéplatz 1, 10117, Berlin, Germany
[3]Department of Medical Immunology, Charité—Universitätsmedizin Berlin, corporate member of Freie Universität Berlin, Humboldt-Universität zu Berlin, and Berlin Institute of Health, Charitéplatz 1, 10117, Berlin, Germany
[4]Institute of Hygiene and Environmental Medicine, Charité—Universitätsmedizin Berlin, corporate member of Freie Universität Berlin, Humboldt-Universität zu Berlin, and Berlin Institute of Health, Charitéplatz 1, 10117, Berlin, Germany
[5]Department of Pediatric Surgery, Charité—Universitätsmedizin Berlin, corporate member of Freie Universität Berlin, Humboldt-Universität zu Berlin, and Berlin Institute of Health, Charitéplatz 1, 10117, Berlin, Germany
[6]Department of Pediatric Respiratory Medicine, Immunology and Critical Care Medicine, Charité—Universitätsmedizin Berlin, corporate member of Freie Universität Berlin, Humboldt-Universität zu Berlin, and Berlin Institute of Health, Charitéplatz 1, 10117, Berlin, Germany
[7]Department of Immunology, Labor Berlin GmbH, Sylter Straße 2, 13353, Berlin, Germany
[8]Charité—Universitätsmedizin Berlin, corporate member of Freie Universität Berlin, Humboldt-Universität zu Berlin, and Berlin Institute of Health, Charitéplatz 1, 10117, Berlin, Germany
[9]Berlin-Brandenburg Center for Regenerative Therapies, Charité—Universitätsmedizin Berlin, corporate member of Freie Universität Berlin, Humboldt-Universität zu Berlin, and Berlin Institute of Health, Charitéplatz 1, 10117, Berlin, Germany
[10]Department of Infectious Diseases and Respiratory Medicine, Charité—Universitätsmedizin Berlin, corporate member of Freie Universität Berlin, Humboldt-Universität zu Berlin, and Berlin Institute of Health, Charitéplatz 1, 10117, Berlin, Germany
*Corresponding author: Department of Cellular Microbiology, Max Planck Institute for Infection Biology, Charitéplatz 1, 10117, Berlin, Germany.
Email: marsman@mpiib-berlin.mpg.de

Abstract

Staphylococcus aureus strains that produce the toxin Panton-Valentine leukocidin (PVL-SA) frequently cause recurrent skin and soft tissue infections. PVL binds to and kills human neutrophils, resulting in the formation of neutrophil extracellular traps (NETs), but the pathomechanism has not been extensively studied. Furthermore, it is unclear why some individuals colonized with PVL-SA experience recurring infections whereas others are asymptomatic. We thus aimed to (1) investigate how PVL exerts its pathogenicity on neutrophils and (2) identify factors that could help to explain the predisposition of patients with recurring infections. We provide genetic and pharmacological evidence that PVL-induced NET formation is independent of NADPH oxidase and reactive oxygen species production. Moreover, through NET proteome analysis we identified that the protein content of PVL-induced NETs is different from NETs induced by mitogen or the microbial toxin nigericin. The abundance of the proteins cathelicidin (CAMP), elastase (NE), and proteinase 3 (PRTN3) was lower on PVL-induced NETs, and as such they were unable to kill *S. aureus*. Furthermore, we found that neutrophils from affected patients express higher levels of CD45, one of the PVL receptors, and are more susceptible to be killed at a low PVL concentration than control neutrophils. Neutrophils from patients that experience recurring PVL-positive infections may thus be more sensitive to PVL-induced NET formation, which might impair their ability to combat the infection.

Keywords: neutrophil extracellular traps, neutrophils, Panton-Valentine leukocidin, *Staphylococcus aureus*, toxin

1. Introduction

Staphylococcus aureus is a widespread Gram-positive pathogen that causes skin and soft tissue infections (SSTI), infections of the osteoarticular system, the airway, and the bloodstream in humans and animals. Nasal colonization with *S. aureus* is found in up to 50% of humans, with strong age variation, and may be asymptomatic provided that skin and mucous membrane barriers are intact.[1,2] Pathogenicity of *S. aureus* strains depends on a variety of virulence factors, among those, pore-forming leukocidins such as Panton-Valentine leucocidin (PVL) that target neutrophils (also called polymorphonuclear leukocytes), and macrophages to evade phagocytosis and intracellular killing (reviewed in Tromp and van Strijp).[3] Over the last 2 decades, an increasing number of outbreaks of SSTIs in close communities[4–12] and in other healthcare settings[13–24] were caused by *S. aureus* strains that produce PVL (PVL-SA).

† These authors contributed equally to this work as joint first authors.
‡ These authors contributed equally to this work as joint senior authors.

Received: March 15, 2023. **Revised:** October 4, 2023. **Accepted:** October 9, 2023. **Corrected and Typeset:** November 30, 2023
© The Author(s) 2023. Published by Oxford University Press on behalf of Society for Leukocyte Biology.
This is an Open Access article distributed under the terms of the Creative Commons Attribution License (https://creativecommons.org/licenses/by/4.0/), which permits unrestricted reuse, distribution, and reproduction in any medium, provided the original work is properly cited.

Downloaded from https://academic.oup.com/jleukbio/article/115/2/222/7379048 by MPI Infection Biology user on 22 April 2024

Although recurrent skin abscesses and furunculosis are often associated with PVL-SA infections, other pathologies are also linked to these strains. These include (1) worldwide reports of severe invasive infections—often complicated by thrombotic events—in previously healthy young individuals,[25–27] (2) breast abscesses in lactating women[28] and transmission to offspring with life-threatening infections,[29] and (3) necrotizing pneumonia,[30] a severe manifestation, often fatal within days of hospital admission.[31,32] In most cases, pneumonia is preceded by viral airway infections, like influenza, parainfluenza[31,32] and SARS-CoV-2.[33–35]

During outbreaks, identical PVL-SA strains have been obtained from individuals with asymptomatic nasal colonization as well as from patients with severe SSTIs or invasive infections,[11] suggesting that host factors may explain susceptibility to, and severity of, PVL-SA infections. Although studies in African Pygmies suggest that genetic variations in *C5ARI* may be associated with PVL-SA colonization,[36] other factors that allow PVL-SA colonization or infections are not known.

The binding specificity of PVL defines both its host- and cell tropism. PVL is a 2-component toxin consisting of LukF-PV and LukS-PV, which bind to the human panleukocyte receptor CD45,[37] and the human complement 5a receptors CD88/C5aR and C5L2, respectively.[38] As a result, human phagocytes are the major target of PVL. Upon binding, the subcomponents heterooligomerize into an octameric membrane spanning pore,[39,40] which drives cell death. Neutrophils express higher levels of both C5a receptors than monocytes[38] and are more sensitive to PVL-mediated killing than both monocytes and macrophages,[41] suggesting that they are the major target of PVL. Importantly, neutrophils are essential for host defense against *S. aureus*,[42] and patients with impaired production of reactive oxygen species (ROS) in phagocytes are particularly sensitive to *S. aureus* infections (see the review by Buvelot et al.).[43] Neutrophils clear invading *S. aureus* through phagocytosis and by undergoing NETosis, a cell death process that results in the formation of neutrophil extracellular traps (NETs). NETs consist of an externalized web of chromatin decorated with antimicrobial peptides and proteases and are toxic to bacteria.[44]

Depending on the stimulus, NET formation may require ROS formation.[45] A common mediator of ROS-dependent NET formation is NADPH oxidase, which produces superoxide (O^{2-}) that spontaneously dismutates to hydrogen peroxide (H_2O_2). Myeloperoxidase (MPO) converts hydrogen peroxide into highly reactive hypochlorous acid. ROS production allows for the release of neutrophil proteases from granules, protease-mediated chromatin decondensation and the final lysis of the plasma membrane.[46–48] Two *S. aureus* toxins that kill neutrophils and result in NET formation are γ-hemolysin AB and PVL.[49–51] Interestingly, *S. aureus* also produces nucleases to escape from NETs.[52] Whether NET formation is a beneficial or detrimental neutrophil response, both for the host as well as for *S. aureus*, remains unclear and may be context dependent.[50]

In this study, we set out to characterize PVL-induced NET formation with the aim to understand its possible contribution to the pathogenesis of PVL-SA infections. We show that PVL-induced NET formation is NADPH oxidase independent. Consistently, neutrophils isolated from chronic granulomatous disease (CGD) patients, which have a mutation in the gene encoding 1 subunit of the NADPH oxidase complex, make NETs in response to this toxin.[53] PVL-induced NETs showed quantitative proteomic differences to NETs produced after PMA or nigericin stimulation. PVL NETs contained a lower abundance of multiple antimicrobial proteins and, in contrast to PMA or nigericin NETs, did not kill *S. aureus*. Given the lack of antimicrobial activity, we asked whether neutrophils from patients with a history of recurrent PVL-SA infection show altered sensitivity to PVL compared with control individuals. Indeed, we found that neutrophils from these patients express higher levels of the PVL receptor CD45 than healthy individuals and make more NETs in response to a low concentration of PVL. Our results suggest that PVL receptor expression may mediate susceptibility to symptomatic *S. aureus* infection and that NET formation induced by this toxin serves as an offensive strategy to preemptively neutralize the neutrophil.

2. Methods

2.1 Neutrophil isolation, experimental conditions, and inhibitors

Human neutrophils were isolated by layering whole blood over Histopaque-1119 (Sigma-Aldrich) followed by a discontinuous Percoll gradient (Amersham Biosciences) as previously described.[46] Alternatively, they were also isolated using the direct human neutrophil isolation kit (EasySep; STEMCELL Technologies) following manufacturer's instructions. All experiments were performed in Seahorse XF RPMI medium (Agilent) supplemented with 2 mM glutamine, 10 mM HEPES, 1 mM glucose, and 0.1% human serum albumin (HSA) at pH 7.4, except where mentioned. The stimuli used to induce NET formation were PMA (Sigma-Aldrich), PVL (equal amounts of *S. aureus* recombinant LukS and LukF [IBT Bioservices], and nigericin [InvivoGen]). We used the following inhibitors: Gö6983 (protein kinase C [PKC] inhibitor; Tocris) BAPTA-AM (Thermo Fisher Scientific), pyrocatechol (Sigma-Aldrich), ABAH (Cayman chemical), neutrophil elastase (NE) inhibitor (NEi) (MedChemExpress), DPI (Calbiochem), AEBSF (Sigma-Aldrich), allopurinol (Sigma-Aldrich), Apamin (Sigma-Aldrich), DNP (Sigma-Aldrich) and FCCP (Abcam).

2.2 ROS measurement

Purified neutrophils were seeded at 10^5 cells per well in a 96-well plate and incubated for 30 min with the indicated inhibitors, followed by incubation for 10 min with 50 μM luminol and 1.2 U/mL horseradish peroxidase at 37 °C prior to stimulation with indicated stimuli. Luminescence was measured over time in a VICTORX luminometer (PerkinElmer).[45]

2.3 Neutrophil lytic cell death assay

A total of 10^5 neutrophils were seeded in a 96-well plate and incubated with the appropriate inhibitors for 30 min, followed by incubation with 50 nM cell-impermeable DNA dye SYTOX Green (Thermo Fisher Scientific) for 5 min at 37 °C, prior to stimulation with indicated stimuli. Fluorescence was recorded once per hour for 4 h using a Fluoroskan Ascent (Thermo Fisher Scientific).

2.4 NET staining

A total of 10^5 neutrophils were seeded on glass coverslips in a 24-well plate and incubated with or without appropriate inhibitors followed by stimulation with indicated stimuli for 4 h at 37 °C. Cells were fixed with 4% paraformaldehyde (PFA) for 20 min at room temperature. Cells were washed with phosphate-buffered saline (PBS), permeabilized with 0.5% Triton X-100 for 1 min, and incubated in blocking buffer (3% normal goat serum, 3% cold water fish gelatin, 1% bovine serum albumin, and 0.05% Tween 20 in PBS) for 30 min. Neutrophils were then stained using antibodies detecting elastase (Merck Millipore; 481001) and a

Downloaded from https://academic.oup.com/jleukbio/article/115/2/222/7379048 by MPI Infection Biology user on 22 April 2024

subnucleosomal complex of histone 2A, histone 2B, and chromatin.[54] The secondary antibodies used were goat anti-mouse Alexa Fluor 488 (Invitrogen; A11029) and goat anti-rabbit Alexa Fluor 647 (Invitrogen; A21245) followed by staining with DAPI (0.1 µg/mL; Invitrogen). Finally, the samples were mounted using antifade mountant (ProLong Diamond Antifade mountant; Thermo Fisher Scientific). Images were acquired using a Leica TCS SP8 confocal microscope.

For live NET imaging, cells were resuspended in Agilent XF RPMI medium at pH 7.4, supplemented with 0.1% human serum albumin, 10 mM Glucose (Sigma-Aldrich), 2 mM L-glutamine (Gibco), 20 mM HEPES (Gibco) 500 nM SYTOX Green (Thermo Fisher Scientific), and 2.5 µM DRAQ5 (Biostatus) and seeded at a density of 5×10^5 cells per well into µ-slide 8 well ibiTreat dishes (ibidi). Cells were stimulated with final concentrations of 100 nM PMA and 10 nM PVL. Images were collected at 2 min intervals on a Leica TCS SP8 confocal microscope equipped with a climate chamber at 37 °C and with a Leica HC PL APO 20×/0.75 IMM CORR CS2 objective using glycerol immersion.[45]

2.5 Mass spectrometry

Human neutrophils from 3 different healthy donors were seeded in 6-well tissue culture plate to a density of 3×10^5 cells per well (Seahorse XF RPMI medium without HSA) and then stimulated with 50 nM PMA, 10 nM PVL, or 15 µM nigericin for 4 h to induce NETs. As a control, neutrophils were incubated in medium for 4 h. Media was carefully removed followed by a wash with fresh media to remove unbound proteins. NETs were collected by treatment with lysis buffer (1% sodium dodecyl sulfate, 50 mM HEPES pH 8, 10 mM TCEP, 40 mM chloroacetamide, and protease-inhibitor cocktail) and subsequent scraping.

All samples were subjected to SP3 sample preparation.[55] Briefly, proteins were denatured, reduced, and alkylated and subsequently digested with Trypsin and Lys-C proteases. TMT 11plex (Pierce) labeling was used for peptide multiplexing and quantification. Samples were mixed, desalted using solid phase extraction (Seppak 1 cm^3/50 mg; Waters), and fractionated using basic reversed phase fractionation on a quaternary Agilent 1290 Infinity II UPLC system equipped with a Kinetex Evo-C18 column (150 × 2.1 mm, 2.6 µm, 100 Å; Phenomenex). Fractions were concatenated into 8 final samples, dried down, and resuspended in 2% acetonitrile, 0.1% trifluoroacetic acid prior to mass spectrometry analysis. All samples were analyzed on an Orbitrap Q Exactive HF (Thermo Fisher Scientific) that was coupled to a 3000 RSLC nano UPLC (Thermo Fisher Scientific). Samples were loaded on a pepmap trap cartridge (300 µm ID ×5 mm, C18; Thermo Fisher Scientific) with 2% acetonitrile, 0.1% trifluoroacetic acid at a flow rate of 20 µL/min. Peptides were separated over a 50 cm analytical column (Picofrit, 360 µm OD, 75 µm ID, 10 µm tip opening, noncoated; New Objective) that was packed in house with Poroshell 120 EC-C18, 2.7 µm (Agilent). Solvent A consisted of 0.1% formic acid in water. Elution was carried out at a constant flow rate of 250 nL/min using a 180-min method: 8% to 33% solvent B (0.1% formic acid in 80% acetonitrile) within 120 min, 33% to 48% solvent B within 25 min, and 48% to 98% buffer B within 1 min, followed by column washing and equilibration. The mass spectrometer was operated in data-dependent acquisition mode. The MS1 survey scan was acquired from 375 to 1500 m/z at a resolution of 120 000. The top 10 most abundant peptides were isolated within a 0.7 Da window and subjected to higher-energy collisional dissociation fragmentation at a normalized collision energy of 32%. The automatic gain control target was set to 2×10^5 charges, allowing a maximum injection time of 78 ms. Product ions were detected in the Orbitrap at a resolution of 45 000. Precursors were dynamically excluded for 45 s. Raw files were processed with Proteome Discoverer 2.3 (Thermo Fisher Scientific) using SEQUEST HT for peptide identification. Peptide-spectrum matches were filtered to a 1% false discovery rate level using Percolator employing a target/decoy approach. The protein false discovery rate was set to 1%. Further data processing was carried out in R (R Foundation for Statistical Computing [version 3.6.1]) and Perseus (version 1.6.2.3). Only proteins identified with at least 2 peptides were included in the analysis. All contaminant proteins were filtered out. A 3-step normalization procedure was applied. First, the total intensity of each TMT channel was normalized to correct for mixing errors. Next, the common channel in both TMT sets was used for internal reference scaling[56] in order to correct for batch effects. Afterwards the data was normalized applying trimmed mean of M values using the edgeR package in R.[57] Proteins were filtered on those detected in at least 2 of 3 replicate experiments. Remaining undetected (NA) values were replaced with the sample-wise minimum abundance as an estimation of the limit of detection. Differential protein abundances were calculated using the limma package in R.[58] Principal component analysis and calculation of Euclidean distance between proteome samples were performed using scaled log2(abundance) values.

2.6 NET killing assay

Purified neutrophils were seeded at 10^6 cells per well in a flat-bottom 96-well plate. NET formation was induced with 100 nM PVL, 100 nM PMA, or 30 µM nigericin for 4 h at 37 °C. If applicable, residual phagocytosis was subsequently blocked with 10 µg/mL cytochalasin B (Abcam) for 15 min. *S. aureus* (USA300) in mid-logarithmic phase was added at a multiplicity of infection of 2 in RPMI with 10% human serum (Sigma-Aldrich). Bacteria were spun down for 5 min at 800 *g* and incubated for 1 h at 37 °C. After incubation, NETs were treated with 2 U micrococcal nuclease (TaKaRa Bio) for 10 min at room temperature. Samples were resuspended, serially diluted in Dulbecco's phosphate-buffered saline and plated on trypticase soy agar plates. The plates were incubated overnight at 37 °C and colony-forming units were counted. Bacterial viability was expressed as a percentage of bacteria incubated for 1 h without NETs.

For DNA quantification, NETs were induced as described previously and digested with 2 U micrococcal nuclease for 10 min at room temperature, and subsequently with 0.5 mg/mL of proteinase K (Invitrogen) for 1 h at 50 °C. The samples were vortexed and the DNA concentration was measured on Nanodrop 2000 spectrophotometer (Thermo Fisher Scientific).

2.7 Neutrophil markers

A total of 1×10^6/mL neutrophils were fixed for 15 min using 4% PFA and washed to PBS supplemented with 0.1% HSA. Cells were incubated with anti-CD63-PE, anti-CD66b-APC (Miltenyi Biotec), 5 µg/mL anti-CD45-Alexa Fluor 647 (Santa Cruz Biotechnology), 10 µg/mL CD88 (S5/1)-FITC (Santa Cruz Biotechnology), and 10 µg/mL anti-human C5L2-APC (BioLegend) antibodies for 30 min in the dark, washed thereafter with PBS supplemented with 0.1% HSA, and measured on a CytoFLEX (Beckman Coulter) or MACSQuant (Miltenyi Biotec).

2.8 Patient and control characteristics

Patient demographic and clinical data are summarized in Supplementary Table 2. Control individuals were matched for

Downloaded from https://academic.oup.com/jleukbio/article/115/2/222/7379048 by MPI Infection Biology user on 22 April 2024

sex and age. PVL-positive status was confirmed for all patients. All study participants provided written informed consent and were free of infections at the time of blood withdrawal. The study was approved by the local Ethics committee (EA2/003/19). Healthy control samples were collected according to the approval and guidelines of the local ethics committee (EA1/0104/06).

2.9 Statistical analysis

Analysis of differential protein abundance was performed in limma (Linear Models for Microarray data) in R, which has been shown to outperform t tests in detecting significant changes in protein abundance.[59] Protein-wise linear models were fit and batch-corrected using the formula (0 + condition + batch), and significant changes in abundance were tested using an empirical Bayes moderated t statistic with Benjamini-Hochberg correction. Changes in abundance were considered significant at an absolute log2 fold change > 1, and an adjusted P value < 0.01. Euler diagrams of significant changes across samples were visualized with the eulerr package.[60] Significant proteins were clustered by pattern across conditions using k-means clustering with indicated number of clusters. Heatmaps were produced using pheatmap package.[61]

R scripts for proteome analysis and visualization can be found in the supporting zip document.

Data are represented as mean ± SD unless otherwise stated.

3. Results

3.1 PVL induces NETs independent from ROS

To further our understanding of the role of PVL toxin in PVL-SA pathogenesis, we verified[50,51] and further characterized PVL-induced NET formation. NADPH oxidase–dependent superoxide formation is essential in NETs induced by some stimuli,[45] prompting us to investigate the NETosis pathway initiated by PVL. We first tested superoxide generation in healthy primary neutrophils stimulated with different concentrations of PVL or PMA, a well-characterized mitogen that induces NADPH oxidase–dependent NETosis.[63] PVL stimulation resulted in weak superoxide production at all concentrations (Fig. 1A). In contrast, PMA induced a significant superoxide burst.

We quantified ROS production as well as NET formation in neutrophils from CGD patients. As expected, CGD neutrophils failed to generate superoxide in response to PVL or PMA (Fig. 1B). However, unlike PMA, PVL induced extracellular DNA release (Fig. 1C) and NET formation (Fig. 1D and Supplementary Videos 1 and 2) in CGD neutrophils. These data show that while PVL stimulation weakly activates NADPH oxidase, NET formation is independent from the produced ROS.

Given the known involvement of various neutrophil proteins in NET formation, we asked if PVL-induced NET formation could be blocked pharmacologically by the PKC inhibitor Gö6983, the calcium chelator BAPTA-AM, the NADPH oxidase inhibitor DPI, the ROS scavenger pyrocatechol, the myeloperoxidase inhibitor ABAH, the neutrophil elastase inhibitor NEi, or the pan serine protease inhibitor AEBSF (Fig. 1E, F, and H). We observed that PKC inhibitor weakly inhibited NET formation induced by 1 nM PVL (Fig. 1E), while none of the other inhibitors, including inhibitors of ROS-producing enzymes (DPI and ABAH) or ROS scavengers (pyrocatechol), blocked NET formation induced by 1 or 10 nM PVL (Fig. 1E, F, and H). Notably, neutrophils pretreated with NEi or AEBSF and stimulated with 1 nM PVL formed smaller NETs (Fig. 1H). These data suggest that PVL-mediated NET formation is ROS and protease independent. As a control, we confirmed[45] that PMA-induced NET formation was blocked by all inhibitors tested (Fig. 1G, H).

Mazzoleni et al.[51] suggested that small conductance calcium-activated potassium (SK) channels and alternative ROS sources, such as mitochondria or xanthine oxidase, mediate PVL-induced NET formation. To verify this, we pretreated neutrophils with the xanthine oxidase inhibitor allopurinol, the SK channel inhibitor apamin, and the mitochondrial uncouplers DNP and FCCP, before stimulating with either PMA or PVL. The SK channel inhibitor NS8593 was toxic to neutrophils in our hands and was excluded from our experiments. At 1 nM, but not at 10 nM PVL stimulation, allopurinol inhibited NET formation, while mitochondrial uncoupling with FCCP partially inhibited NET formation. (Supplementary Fig. 1A, B). These findings were supported by confocal imaging (Supplementary Fig. 1D). None of the inhibitors affected PMA-induced NET formation (Supplementary Fig. 1C). Given that PVL induces NET formation in CGD patients despite a complete lack of ROS (Fig. 1B), and the inability of the ROS scavenger pyrocatechol to inhibit PVL-induced NET formation, the inhibition of NETs by allopurinol treatment or mitochondrial uncoupling appears to be independent of ROS production. This is further supported by the observation that DPI, which not only inhibits NADPH oxidase, but all flavin-containing proteins including xanthine oxidase[64] and mitochondrial complex I,[65] did not block PVL-induced NET formation (Fig. 1E, F). Finally, the inability of ROS-targeting inhibitors to block NET formation induced by 10 nM PVL indicates that PVL-induced NET formation is independent from ROS production.

3.2 PVL-induced NETs lack enrichment of key antimicrobial proteins

Because PVL induces NETs through a noncanonical pathway, we hypothesized that the resulting NETs may have different protein compositions. We therefore analyzed the proteomes of NETs induced by PVL, PMA, and the NADPH oxidase–independent NET inducer nigericin.[45] We analyzed NETs from 3 independent donors by quantitative mass spectrometry and compared them with the proteome of unstimulated neutrophils. Principal component analysis revealed that PVL-, PMA- and nigericin-induced NETs each have distinct proteomes (Fig. 2A). Interestingly, PVL NETs appear to cluster between naïve neutrophils and NETs induced by PMA and nigericin, suggesting that their proteome composition is intermediate between naïve cells and classical NETs. Measurement of the Euclidean distance between samples confirmed that the PVL-NET proteome is less distinct from naïve neutrophils than that of PMA- or nigericin-induced NETs (Supplementary Fig. 2A).

We detected 2458 distinct proteins in the combined NET samples (present in at least 2 of 3 replicate experiments). To examine which proteins are driving the differences between the NET proteomes, we performed a differential enrichment analysis using a 2-fold change in protein abundance with an adjusted P value below 0.01 as a cutoff. We found significant differences in relative protein abundance between all 3 NET stimuli when compared with naïve neutrophils (Fig. 2B and Supplementary Fig. 2A). Fewer differentially abundant proteins (DAPs) were detected between PVL-induced NETs and naïve polymorphonuclear leukocytes (194 significant) compared with PMA-induced (449) and nigericin-induced (670) NETs. These data suggest that the specific enrichment or depletion of proteins during NET formation is lower or incomplete in PVL-treated neutrophils.

Downloaded from https://academic.oup.com/jleukbio/article/115/2/222/7379048 by MPI Infection Biology user on 22 April 2024

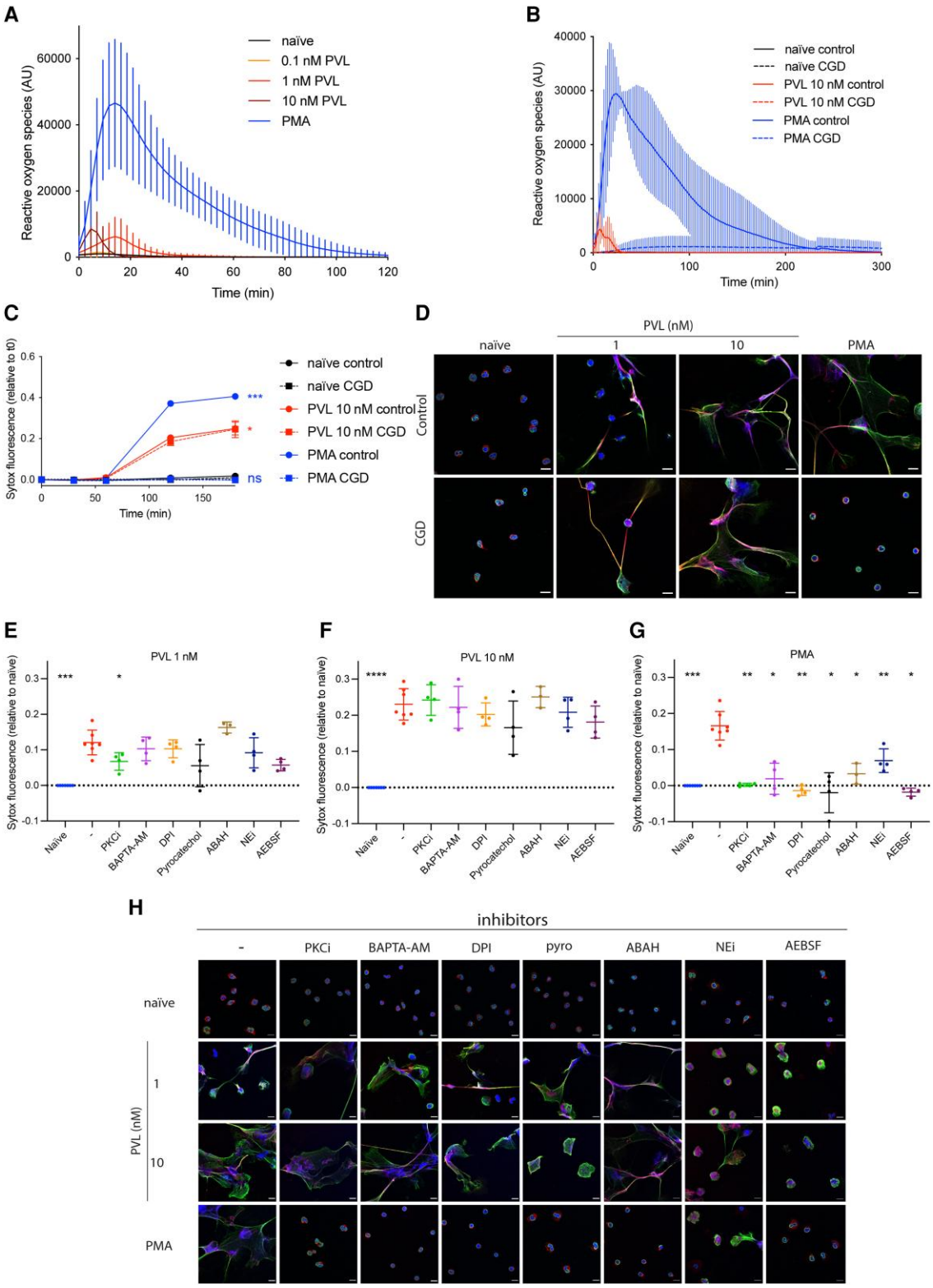

Fig. 1. PVL induces ROS-independent NET formation. (A, B) ROS formation was quantified in control (A: n = 14, B: n = 3) or CGD human (n = 3) primary neutrophils stimulated with PMA (50 nM) or PVL (0.1 nM, 1 nM or 10 nM). (C) Control or CGD neutrophils were stimulated with PMA (50 nM) or PVL (10 nM) for 3 h, and cell death was quantified using the cell-impermeable DNA dye SYTOX Green. Indicated is SYTOX Green fluorescence relative to $t = 0$ min. (D) Representative confocal microscopy images of control and CGD patient neutrophils either naïve or stimulated with PMA (50 nM) or PVL (1 nM or 10 nM) and stained for DNA (blue), NE (red), and chromatin (green). The scale bar represents 10 μm. (E–G) Healthy human neutrophils were treated with PKC inhibitor Gö6983 (1 μM), BAPTA-AM (10 μM), DPI (1 μM), pyrocatechol (30 μM), ABAH (500 μM), NEi (20 μM), and AEBSF (100 μM) for 30 min, before stimulating with (E) PVL 1 nM, (F) PVL 10 nM, or (G) PMA 50 nM for 4 h. We quantified cell death with SYTOX Green and the fluorescence signal relative to naïve is indicated. (H) Representative confocal microscopy of naïve neutrophils or after stimulation with PMA or PVL (1 nM or 10 nM) in the presence or absence of indicated inhibitors, and stained for DNA (blue), NE (red), and chromatin (green). The scale bar represents 10 μm. (C) Two-way analysis of variance with Tukey's post hoc test. $^{*}P < 0.05$, $^{***}P < 0.001$. (E–G) Mean ± SD of 4 independent experiments. $^{*}P < 0.05$, $^{**}P < 0.01$, $^{***}P < 0.001$, $^{****}P < 0.0001$, 1-way analysis of variance with Dunnett's multiple comparison test. ns = not significant.

Downloaded from https://academic.oup.com/jleukbio/article/115/2/222/7379048 by MPI Infection Biology user on 22 April 2024

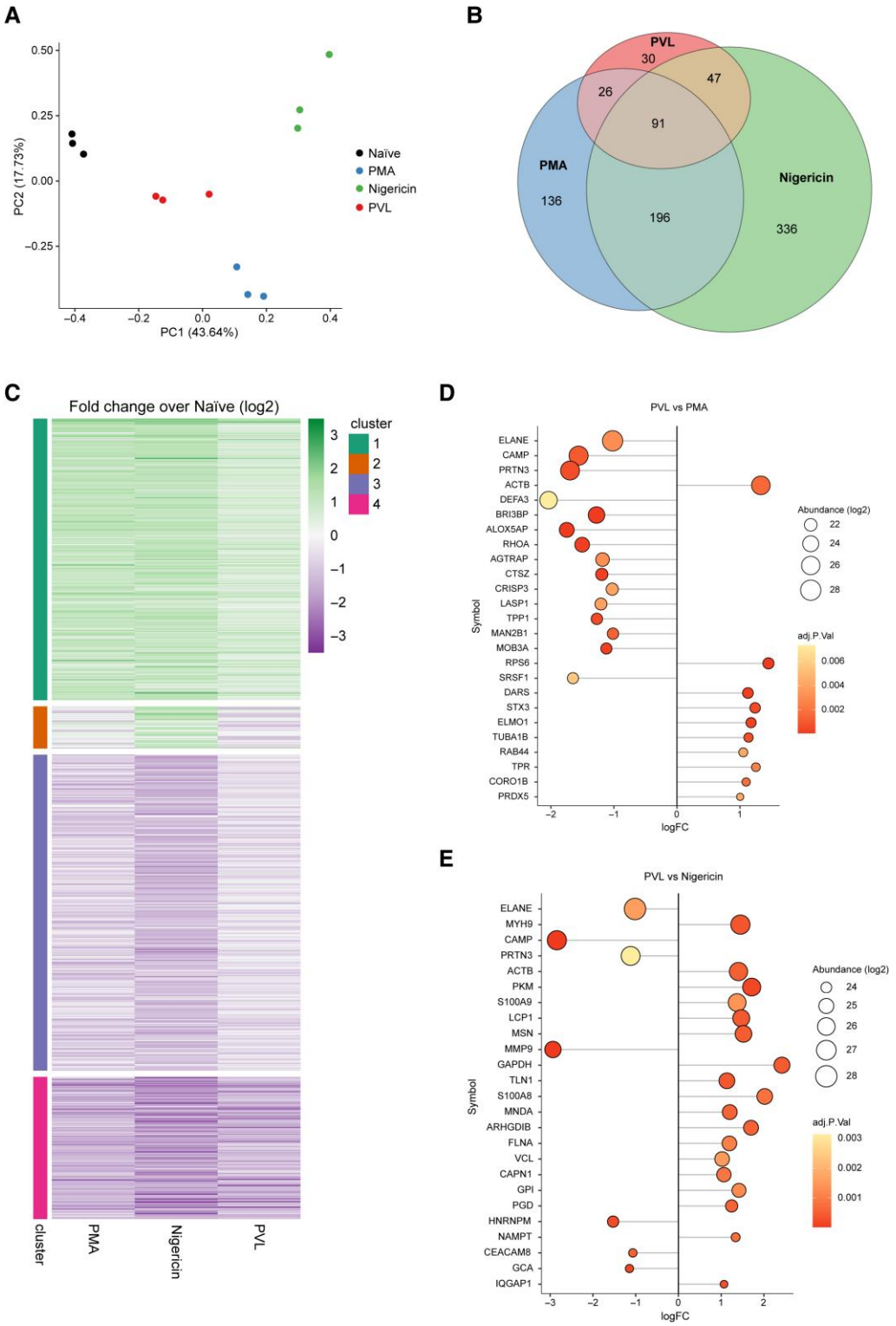

Fig. 2. NET proteome assembly is different in PVL-induced NETs. (A) Principal component analysis of the proteomes of naïve neutrophils, and PVL-induced (10 nM), PMA-induced (50 nM), and nigericin-induced (15 μM) NETs. Analysis was performed on scaled log2-abundance of all proteins detected in at least 2 of 3 replicates. (B) Euler diagram showing the number and distribution of significant differentially abundant peptides (logFC > 1, adjusted $P < 0.01$) on NETs compared with naïve neutrophils. Areas are proportional to DAP set size. (C) Clustered heatmap showing fold change (log2) values on each NET sample compared with naïve neutrophils of significant DAPs from panel B. Clustering was performed by k-means algorithm with k = 4 clusters. (D, E) Top 25 most abundant DAPs that are significantly differentially abundant on PVL-induced NETs compared with PMA-induced (D) and nigericin-induced NETs (E). Point size and fill color represent average abundance across samples and adjusted *P* value, respectively. Proteomes were made from n = 3 samples per condition from independent donors. DAP significance for each comparison was determined by a threshold of |[log2 fold change]| > 1 and adjusted *P* value < 0.01.

Downloaded from https://academic.oup.com/jleukbio/article/115/2/222/7379048 by MPI Infection Biology user on 22 April 2024

Examination of the fold changes of NET-specific DAPs revealed that most DAPs have the same pattern of enrichment or depletion across all types of NETs compared with naïve neutrophils (459 with negative logFC, 294 positive logFC) (Fig. 2C). Regression of global DAP fold changes (Supplementary Fig. 2B) revealed that though most proteins have the same enrichment pattern across NETs, the fold-changes are reduced in PVL- compared with PMA- and nigericin-induced NETs (slopes = 0.64 and 0.49, respectively), while PMA and nigericin NETs have equivalent DAP fold-changes (slope = 1).

K-means clustering of DAP fold change patterns supported this trend and further identified a cluster of proteins specifically enriched on nigericin induced NETs (Fig. 2C cluster 2, orange; Supplementary Table 1). To look more closely at the differences between PVL-induced NETs and PMA- or nigericin-induced NETs, we performed pairwise comparisons between PVL and PMA or PVL and nigericin (Supplementary Fig. 2C, and D) and ranked the 25 most abundant DAPs (Fig. 2D and E, respectively). Among these, key neutrophil proteins such as NE (ELANE), PRTN3, and CAMP were all less abundant on PVL-induced NETs compared with PMA- or nigericin-induced NETs. In contrast, we found cytoskeleton proteins such as actin (ACTB), myosin (MYH9), and tubulin (TUBA1B) to be more enriched on PVL NETs. Our data suggest that PVL induces NETs with a different NET proteome assembly when compared with PMA or nigericin, resulting in a lack of enrichment of key antimicrobial proteins on PVL NETs.

3.3 PVL-induced NETs are less bactericidal

Given the differential enrichment of antimicrobial proteins in PVL- compared with PMA- and nigericin-induced NETs, we hypothesized that their bactericidal activity may be different. We incubated methicillin-resistant *S. aureus* (MRSA) with either PVL-, PMA-, or nigericin-induced NETs for 1 h, harvested the bacteria, and quantified the surviving colony forming units. PVL-induced NETs did not kill MRSA, while PMA- and nigericin-induced NETs did (Fig. 3A). We verified that all stimuli at these concentrations released similar amounts of NETs by nanodrop DNA quantification (Fig. 3B). To exclude a possible contribution of killing through phagocytosis we performed the same experiment in the presence of cytochalasin B. We did not observe a difference in antimicrobial activity upon inhibition of phagocytosis, indicating that NETs were solely responsible for the killing (Supplementary Fig. 3). These results show that PVL NETs have a lower antimicrobial potential against MRSA than PMA- or nigericin-NETs.

3.4 PVL induces NETs efficiently in neutrophils from patients with recurrent PVL-SA infections

The lack of antimicrobial activity of PVL NETs prompted us to ask whether neutrophils from patients that experience recurrent PVL-SA infections show altered responses to PVL that may help to explain the patients' increased susceptibility to infection. We quantified NET formation in response to 0.1, 1, and 10 nM PVL in patients and control individuals using a cell impermeable DNA dye. Interestingly, 0.1 nM PVL killed neutrophils isolated from patients more efficiently than neutrophils isolated from healthy control individuals (Fig. 4A). Patient and control neutrophils were equally susceptible to make NETs in response to PMA.

Given the binding specificity of PVL we checked the expression of CD45, CD88, and C5L2, as well as the neutrophil activation markers CD63 and CD66b, on control and patient neutrophils by flow cytometry. Patient neutrophils expressed higher levels of CD45 ($P = 0.000473$), and there was no difference in CD88. Furthermore, a subset of patients expressed increased C5L2 levels compared with control neutrophils (Supplementary Fig. 4A), but this trend was not consistent for all patients (Fig. 4B). Interestingly, the difference in expression of C5L2 and possibly CD45 in patients compared with control individuals correlated with the difference in NET formation in response to 0.1 nM PVL ($\rho = 0.4491$ for CD45, $\rho = 0.7105$ for C5L2) (Fig. 4C, D). Differences in expression levels of CD88, CD63, or CD66b did not correlate with differences in NET formation (Supplementary Fig. 4B–D).

Taken together, our data suggest that neutrophils from patients with recurrent PVL-SA infections express higher levels of the PVL receptor CD45 and may be more sensitive to PVL-induced NET formation at low PVL concentrations when compared with control neutrophils.

4. Discussion

In the past few decades, PVL has emerged as an important virulence factor in community acquired SA infections. Interestingly, human host factors that mediate susceptibility or severity of PVL-SA infections are not known. To further our understanding of the contribution of PVL to PVL-SA pathogenesis, we set out to characterize PVL-induced NET formation. PMA or *Candida albicans* induce NET formation, which is ROS dependent and is blocked by compounds that scavenge ROS or inhibit ROS.[45] Other stimuli, like nigericin and calcium ionophores, induce NETs through a ROS independent mechanism.[45] We identified that PVL induces the formation of NETs independently of NADPH oxidase and MPO activity, 2 enzymes that produce ROS. This is evidenced by 2 observations: (1) CGD neutrophils do not produce ROS upon stimulation with PVL, but make NETs; and (2) DPI, an inhibitor of flavin-containing proteins such as NADPH oxidase, xanthine oxidase,[64] and cytochrome C,[65,66] the ROS scavenger pyrocatechol, and the MPO inhibitor ABAH all fail to inhibit PVL-induced NET formation.

A recent study by Mazzoleni et al.[51] suggested that ROS derived from mitochondria or xanthine oxidase are involved in PVL-induced NET formation. We observed that treatment with DNP or FCCP, as well as xanthine oxidase inhibition by allopurinol, partly inhibited PVL-induced NET formation. Xanthine oxidoreductase consists of 2 isoforms, xanthine oxidase and xanthine dehydrogenase. Allopurinol inhibits both isoforms, which affects purine metabolism. Moreover, allopurinol itself generates superoxide radicals upon inhibition of xanthine oxidase.[67] Therefore, its inhibitory effect on PVL-induced NET formation may be independent from xanthine oxidase inhibition or ROS formation. How allopurinol exerts its inhibitory effects on PVL-induced NET formation is still unclear. Furthermore, given that both DPI and the ROS scavenger pyrocatechol were unable to inhibit PVL-induced NET formation, we hypothesize that the inhibitory effect of allopurinol and FCCP is independent from their effects on ROS production. Notably, inhibition of NET formation by these inhibitors was seen at 1 nM PVL but was lost when stimulating with 10 nM PVL. It may be that PVL at high concentrations is able to induce NET formation without the involvement of neutrophil components interrogated by the inhibitors used in our study, while at low PVL concentrations some components may contribute to NET formation.

Neutrophil proteases were not essential for PVL-induced NET formation, although we did observe that formed NETs appeared smaller upon protease inhibition. Neutrophil elastase is known to contribute to chromatin decondensation during NADPH

Downloaded from https://academic.oup.com/jleukbio/article/115/2/222/7379048 by MPI Infection Biology user on 22 April 2024

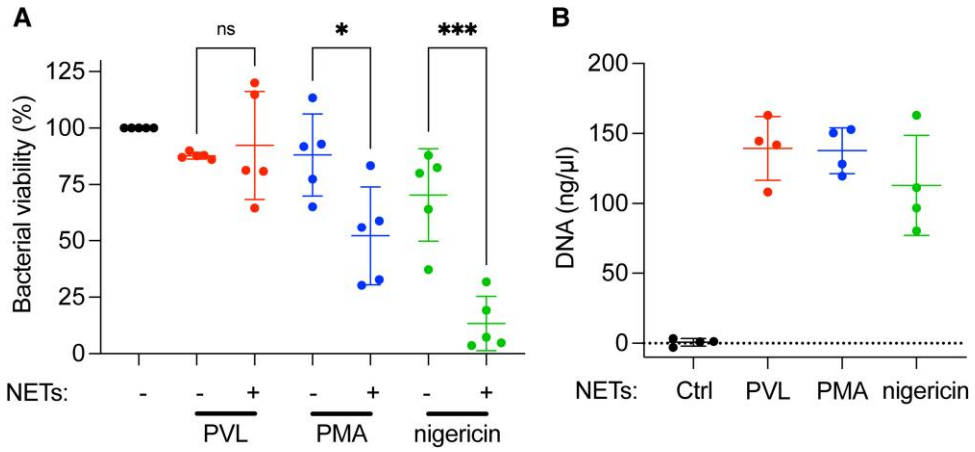

Fig. 3. PVL-induced NETs do not kill MRSA. (A) Primary human neutrophils were stimulated with PVL (100 nM), PMA (100 nM), or nigericin (30 µM) for 4 h to induce NETs. MRSA was incubated with these NETs for 1 h and colony-forming units was quantified after overnight incubation on TSA plates. Bacterial viability is expressed as a percentage of colony-forming units normalized to MRSA incubated in the absence of NETs. (B) The DNA content of PVL-, PMA-, and nigericin-induced NETs at 4 h was quantified by spectrophotometry. (A) Mean ± SD of 5 independent experiments. *$P < 0.05$, *** $P < 0.001$, 1-way analysis of variance. (B) Mean ± SD of 4 independent experiments. ns = not significant.

oxidase–dependent NETosis[47,68] and this decondensation may occur during PVL-mediated NET formation as well. Although PAD4-mediated histone citrullination has been suggested to be involved in NADPH oxidase-independent NET formation, others have excluded its involvement in driving PVL-induced NET formation.[51]

Interestingly, different NETosis mechanisms lead to NETs with specific compositions. We found differences in protein abundances of NETs induced by PVL, PMA, or nigericin, and the proteome of PVL NETs specifically appears to be less distinct from that of unstimulated neutrophils. Several antimicrobial proteins are less abundant in PVL-induced NETs, when compared with PMA- or nigericin-induced NETs. In contrast, cytoskeletal proteins are more abundant on PVL NETs. A previous report also identified a similar enrichment of cytoskeletal proteins in spontaneously lysed neutrophils.[69] Given PMA- or nigericin-induced NET formation involves an intracellular release of granular components,[68] this mixing of the bag may allow for efficient tethering of granular components to the chromatin backbone and degradation of the cytoskeleton. Cell lysis occurs 2 to 3 h after stimulation with PMA, while PVL-induced NET formation occurs swiftly, with cell lysis occurring within the first 2 h after stimulation. We speculate that granular components may be lost to the extracellular environment during this rapid lysis, resulting in a less bactericidal NET. These data suggest that NETs induced by different stimuli may display different functional characteristics. Leukocidins such as PVL may have evolved to elicit a harmless form of NET formation to promote survival of the invading bacteria.

We hypothesized that the lack of antimicrobial activity of PVL NETs might contribute to PVL-SA pathogenesis and asked whether neutrophils from patients that experience recurrent PVL-SA infections show unusual responses to PVL. We identified increased NET formation in patient neutrophils upon stimulation with a low PVL concentration, and a higher expression of CD45 and potentially C5L2, 2 of the toxin's receptors, in patient neutrophils compared with healthy control individual neutrophils. Furthermore, the increase in CD45 and C5L2 expression correlated with more NET formation induced by PVL.

LukS-PV and LukF-PV have different binding affinities to their respective receptors (C5L2 and CD88 for LukS-PV, CD45 for LukF-PV), and the low binding affinity of LukF-PV to CD45 suggests that varying expression levels of CD45 are unlikely to modulate pore formation.[37] In contrast, LukS-PV binding affinity to CD88 or C5L2 is much higher, and therefore their expression may modulate sensitivity to PVL toxin. Given that neutrophils express C5L2 less abundantly than CD88, it was surprising to find that differential expression of C5L2 correlates with an increased sensitivity of patient neutrophils to PVL.[38] However, the affinities of LukS-PV binding to CD88 and C5L2 have never been compared, and the relative contribution of C5L2-binding to PVL mediated cell death is therefore not known. Whether there is a genetic predisposition in patients with recurrent PVL-SA remains to be determined and we are currently investigating avenues to study this.

CD88 localizes to the plasma membrane, rendering it accessible for extracellular PVL toxin. However, there are conflicting reports on the localization of C5L2 because it has been detected both intracellularly and on the plasma membrane.[70,71] We detected C5L2 on the plasma membrane through flow cytometry, suggesting that the expression is not exclusively intracellular. However, much is unknown concerning the regulation of C5L2 and CD88 expression and receptor shuttling, and it is unclear how this regulation might affect targeting by PVL.[70,71]

Pore formation by PVL is described to exert various cellular effects such as intracellular calcium flux, ATP release into the extracellular environment, induction of apoptosis, and cellular lysis.[72] These various phenotypes likely depend on the toxin concentration a cell encounters. We therefore characterized NET formation at different PVL concentrations and observed robust NET formation upward of 1 nM PVL. In clinical samples from PVL-SA patients, median levels of PVL toxin were previously found to be 0.42 µg/mL (~11 nM) with a range of 0 to 399 µg/mL, which suggests that NET induction may be expected in these patients,[73] notwithstanding the difficulty of predicting PVL potency in vivo.

S. aureus produces a range of toxins, of which some, such as hIgAB and hIgCD, have lytic properties as well.[74] Although we find differences in the expression level of receptors for LukF and LukS, and detected a correlation of these expression levels with the sensitivity of neutrophils to produce NETs, we cannot exclude that expression levels of receptors for other *S. aureus* toxins may contribute as well to the overall sensitivity of neutrophils to produce NETs in response to a *S. aureus* infection. Alternatively, some *S. aureus* toxins, such as peptide-spectrum matches, drive cellular lysis through lysis of the phagolysosome instead of the plasma membrane,[75]

Downloaded from https://academic.oup.com/jleukbio/article/115/2/222/7379048 by MPI Infection Biology user on 22 April 2024

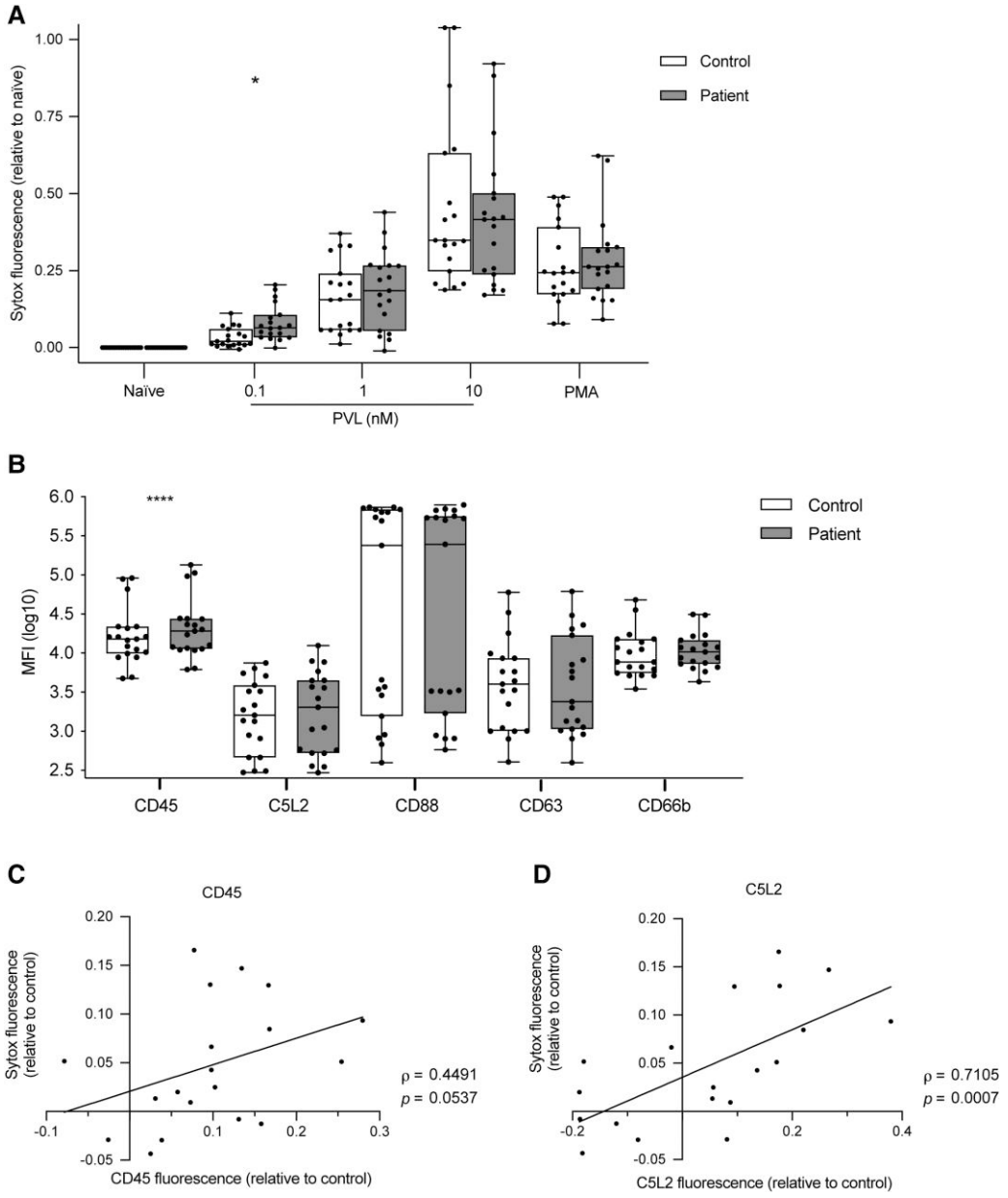

Fig. 4. Neutrophils from patients with recurrent PVL-SA infections make more NETs in response to PVL and express more CD45 than neutrophils from healthy donors. (A) Purified primary neutrophils from patients experiencing recurrent PVL-SA infections (n = 19) and healthy control individuals (n = 19) were either left untreated or stimulated with PMA (50 nM) or PVL (0.1 nM, 1 nM, or 10 nM) for 4 h, and cell death was quantified by adding the cell-impermeable DNA dye SYTOX Green and measuring fluorescence. The boxplot indicates SYTOX fluorescence relative to naïve neutrophils at 4 h. (B) CD45, C5L2, CD88, CD63, and CD66b were immunolabelled on neutrophils from patients and healthy control individuals. The fluorescence was measured and indicated as log-transformed mean fluorescence intensity (MFI). (C) CD45 or (D) C5L2 fluorescence of patient neutrophils relative to control neutrophils was plotted against SYTOX fluorescence of patient neutrophils relative to control neutrophils after incubation with 0.1 nM PVL for 4 h. (A) Unpaired Wilcoxon signed rank test with Bonferroni post hoc test, $^{*}P < 0.05$. (B) Paired *t* test, $^{****}P < 0.0001$. (C, D) Spearman's correlation test in which the coefficient of correlation (ρ) and probability (*P*) are indicated. A best-fit line indicates the trend.

which may drive entirely different cellular responses. Our results strengthen the premise of future studies into neutrophil-specific factors that modulate sensitivity to *S. aureus* toxin subcomponents. In specific, different combinations of *S. aureus* toxin subcomponents may modulate different cellular responses.

NETs have at least 3 described functions: they are antimicrobial,[44] procoagulant,[76] and activate the immune system.[77,78] PVL-SA infections may be associated with a higher risk for thrombotic events. In addition to being less antimicrobial, it would be interesting to investigate if PVL-induced NETs also differ in their procoagulant or immune activation functions.

In conclusion, our observation of (1) differentially expressed PVL receptors in individuals with recurrent or severe PVL-SA infections and (2) functionally different NET formation after neutrophil exposure to PVL in contrast to other stimuli may explain specific clinical features and interindividual differences in PVL-SA infections. We propose that overexpression of PVL receptors might make an individual's neutrophils more prone to this disarmed NET formation, preventing efficient clearance of the invading bacteria. In turn, this could provide a competitive advantage to PVL-SA, facilitating colonization and recurrent infections. Further investigations are necessary to verify this

Downloaded from https://academic.oup.com/jleukbio/article/115/2/222/7379048 by MPI Infection Biology user on 22 April 2024

finding and find potential treatment or prevention strategies for these infections.

Acknowledgments

The authors thank Christian Frese from the Proteomics Research Platform at the Max Planck Unit for the Science of Pathogens for proteomic analysis. The authors thank Alf Herzig for visualizing PVL-induced NET formation in healthy and CGD neutrophils in real time by confocal microscopy. They thank Drs. Dhiren Patel and Garth Burns for their collegial support.

Author contribution

H.J., A.Z., R.K., and G.M. designed the study. H.J., D.C., and G.M. performed experiments and analyzed the data. H.V.B. and R.K. cared for the patients. A.L., L.G.H., R.L., J.T.S., M.S.S., M.S., and H.V.B. have interpreted the data and revised the manuscript for important intellectual content. C.J.H. analyzed the mass spectrometry data. H.J., A.Z., R.K., and G.M. wrote the manuscript.

Supplementary material

Supplementary materials are available at *Journal of Leukocyte Biology* online.

Conflict of interest statement. None declared.

Data availability

The mass spectrometry proteomics data have been deposited to the ProteomeXchange Consortium via the PRIDE[62] partner repository with the dataset identifier PXD025702.

References

1. Bogaert D, van Belkum A, Sluijter M, Luijendijk A, de Groot R, Rümke HC, Verbrugh HA, Hermans PWM, *et al.* Colonisation by Streptococcus pneumoniae and Staphylococcus aureus in healthy children. *Lancet*. 2004:363:1871–1872. https://doi.org/10.1016/S0140-6736(04)16357-5
2. Wertheim HF, Melles DC, Vos MC, van Leeuwen W, van Belkum A, Verbrugh HA, Nouwen JL, *et al.* The role of nasal carriage in Staphylococcus aureus infections. *Lancet Infect Dis*. 2005:5:751–762. https://doi.org/10.1016/S1473-3099(05)70295-4
3. Tromp AT, van Strijp JAG. Studying staphylococcal leukocidins: a challenging endeavor. *Front Microbiol*. 2020:11:1–8. https://doi.org/10.3389/fmicb.2020.00611
4. Müller-Premru M, Strommenger B, Alikadic N, Witte W, Friedrich AW, Seme K, Kucina NS, Smrke D, Spik V, Gubina M, *et al.* New strains of community-acquired methicillin-resistant Staphylococcus aureus with Panton-Valentine leukocidin causing an outbreak of severe soft tissue infection in a football team. *Eur J Clin Microbiol Infect Dis*. 2005:24:848–850. https://doi.org/10.1007/s10096-005-0048-0
5. Gilbert M, MacDonald J, Louie M, Gregson D, Zhang K, Elsayed S, Laupland K, Nielsen D, Wheeler V, Lye T, *et al.* Prevalence of USA300 colonization or infection and associated variables during an outbreak of community-associated methicillin-resistant Staphylococcus aureus in a marginalized urban population. *Can J Infect Dis Med Microbiol*. 2007:18:357–362. https://doi.org/10.1155/2007/597123
6. Carré N, Sillam F, Dabas J-P, Herbreteau N, Pinchon C, Ortmans C, Thiolet J-M, Vandenesch F, Coignard B, *et al.* Staphylococcus aureus carrying Panton-Valentine leukocidin genes nasal colonization and skin infection: screening in case of outbreak in a school environment. *Med Mal Infect*. 2008:38:483–488. https://doi.org/10.1016/j.medmal.2008.06.025
7. Carré N, Herbreteau N, Askeur N, Dabas J-P, Sillam F, Pinchon C, Bes M, Tristan A, Vandenesch F, *et al.* Outbreak of skin infections due to Staphylococcus aureus carrying Panton-Valentine leukocidin genes in pupils and their relatives. *Med Mal Infect*. 2011:41:364–371. https://doi.org/10.1016/j.medmal.2010.12.017
8. Higashiyama M, Ito T, Han X, Nishiyama J, Tanno A, Wada T, Funaoka Y, Yoshida Y, Mikita K, Ogawa T, *et al.* Trial to control an outbreak of Panton-Valentine leukocidin-positive methicillin-resistant Staphylococcus aureus at a boarding school in Japan. *Am J Infect Control*. 2011:39:858–865. https://doi.org/10.1016/j.ajic.2011.02.010
9. Bourigault C, Corvec S, Brulet V, Robert P-Y, Mounoury O, Goubin C, Boutoille D, Hubert B, Bes M, Tristan A, *et al.* Outbreak of skin infections due to panton-valentine leukocidin-positive methicillin-susceptible Staphylococcus aureus in a French prison in 2010-2011. *PLoS Curr*. 2014:6:ecurrents.outbreaks.e4df88f057fc49e2560a235e0f8f9fea. https://doi.org/10.1371/currents.outbreaks.e4df88f057fc49e2560a235e0f8f9fea
10. Couvé-Deacon E, Tristan A, Pestourie N, Faure C, Doffoel-Hantz V, Garnier F, Laurent F, Lina G, Ploy M-C, *et al.* Outbreak of Panton-valentine leukocidin–associated methicillin-susceptible staphylococcus aureus infection in a rugby team, France, 2010–2011. *Emerg Infect Dis*. 2016:22:96–99. https://doi.org/10.3201/eid2201.150597
11. Leistner R, Kola A, Gastmeier P, Krüger R, Hoppe P-A, Schneider-Burrus S, Zuschneid I, Wischnewski N, Bender J, Layer F, *et al.* Pyoderma outbreak among kindergarten families: association with a Panton-Valentine leukocidin (PVL)-producing S. aureus strain. Becker K, editor. *PLoS One*. 2017:12:e0189961. https://doi.org/10.1371/journal.pone.0189961
12. Ismail H, Govender NP, Singh-Moodley A, van Schalkwyk E, Shuping L, Moema I, Feller G, Mogokotleng R, Strasheim W, Lowe M, *et al.* An outbreak of cutaneous abscesses caused by Panton-Valentine leukocidin-producing methicillin-susceptible Staphylococcus aureus among gold mine workers, South Africa, November 2017 to March 2018. *BMC Infect Dis*. 2020:20:621. https://doi.org/10.1186/s12879-020-05352-5
13. Linde H, Wagenlehner F, Strommenger B, Drubel I, Tanzer J, Reischl U, Raab U, Höller C, Naber KG, Witte W, *et al.* Healthcare-associated outbreaks and community-acquired infections due to MRSA carrying the Panton-Valentine leucocidin gene in southeastern Germany. *Eur J Clin Microbiol Infect Dis*. 2005:24:419–422. https://doi.org/10.1007/s10096-005-1341-7
14. Chi Thuong T, Dac Tho N, Thi Hoa N, Minh Phuong NT, Van Tuan L, Song Diep T, Lindsay J, The Dung N, Van Cam B, Quoc Thinh L, *et al.* An outbreak of severe infections with community-acquired MRSA carrying the panton-valentine leukocidin following vaccination. *PLoS One*. 2007:2:e822. https://doi.org/10.1371/journal.pone.0000822
15. Wagenlehner FME, Naber KG, Bambl E, Raab U, Wagenlehner C, Kahlau D, Höller C, Witte W, Weidner W, Lehn N, *et al.* Management of a large healthcare-associated outbreak of Panton-Valentine leucocidin-positive meticillin-resistant Staphylococcus aureus in Germany. *J Hosp Infect*. 2007:67:114–120. https://doi.org/10.1016/j.jhin.2007.07.006
16. Maltezou HC, Vourli S, Katerelos P, Maragos A, Kotsalidou S, Remoudaki E, Papadimitriou T, Vatopoulos AC, *et al.* Panton-Valentine leukocidin-positive methicillin-resistant Staphylococcus aureus outbreak among healthcare workers in

Downloaded from https://academic.oup.com/jleukbio/article/115/2/222/7379048 by MPI Infection Biology user on 22 April 2024

a long-term care facility. *Int J Infect Dis*. 2009:13:e401–e406. https://doi.org/10.1016/j.ijid.2009.02.004
17. Nagao M, Iinuma Y, Suzuki M, Matsushima A, Takakura S, Ito Y, Ichiyama S, *et al.* First outbreak of methicillin-resistant Staphylococcus aureus USA300 harboring the Panton-Valentine leukocidin genes among Japanese health care workers and hospitalized patients. *Am J Infect Control*. 2010:38:e37–e39. https://doi.org/10.1016/j.ajic.2010.04.214
18. Teare L, Shelley OP, Millership S, Kearns A. Outbreak of Panton-Valentine leucocidin-positive meticillin-resistant Staphylococcus aureus in a regional burns unit. *J Hosp Infect*. 2010:76(3):220–224. https://doi.org/10.1016/j.jhin.2010.04.023
19. Ali H, Nash JQ, Kearns AM, Pichon B, Vasu V, Nixon Z, Burgess A, Weston D, Sedgwick J, Ashford G, *et al.* Outbreak of a South West Pacific clone Panton-Valentine leucocidin-positive meticillin-resistant Staphylococcus aureus infection in a UK neonatal intensive care unit. *J Hosp Infect*. 2012:80:293–298. https://doi.org/10.1016/j.jhin.2011.12.019
20. Pinto AN, Seth R, Zhou F, Tallon J, Dempsey K, Tracy M, Gilbert GL, O'Sullivan MVN, *et al.* Emergence and control of an outbreak of infections due to Panton-Valentine leukocidin positive, ST22 methicillin-resistant Staphylococcus aureus in a neonatal intensive care unit. *Clin Microbiol Infect*. 2013:19:620–627. https://doi.org/10.1111/j.1469-0691.2012.03987.x
21. Garvey MI, Bradley CW, Holden KL, Oppenheim B. Outbreak of clonal complex 22 Panton–Valentine leucocidin-positive methicillin-resistant Staphylococcus aureus. *J Infect Prev*. 2017:18:224–230. https://doi.org/10.1177/1757177417695647
22. Kossow A, Kampmeier S, Schaumburg F, Knaack D, Moellers M, Mellmann A. Whole genome sequencing reveals a prolonged and spatially spread nosocomial outbreak of Panton–Valentine leucocidin-positive meticillin-resistant Staphylococcus aureus (USA300). *J Hosp Infect*. 2019:101:327–332. https://doi.org/10.1016/j.jhin.2018.09.007
23. Panigrahy A, Sinha S, Das BK, Kapil A, Vishnubhatla S, Dhawan B. Staphylococcus aureus colonisation in HIV-infected patients: incidence, risk factors and subsequent skin- and soft-tissue infections. *Indian J Med Microbiol*. 2020:38:444–447. https://doi.org/10.4103/ijmm.IJMM_20_5
24. Ikeuchi K, Adachi E, Sasaki T, Suzuki M, Lim LA, Saito M, Koga M, Tsutsumi T, Kido Y, Uehara Y, *et al.* An outbreak of USA300 methicillin-resistant Staphylococcus aureus among people with HIV in Japan. *J Infect Dis*. 2021:223:610–620. https://doi.org/10.1093/infdis/jiaa651
25. Shallcross LJ, Fragaszy E, Johnson AM, Hayward AC. The role of the Panton-Valentine leucocidin toxin in staphylococcal disease: a systematic review and meta-analysis. *Lancet Infect Dis*. 2013:13:43–54. https://doi.org/10.1016/S1473-3099(12)70238-4
26. Saeed K, Gould I, Esposito S, Ahmad-Saeed N, Ahmed SS, Alp E, Bal AM, Bassetti M, Bonnet E, Chan M, *et al.* Panton–valentine leukocidin-positive Staphylococcus aureus: a position statement from the International Society of Chemotherapy. *Int J Antimicrob Agents*. 2018:51:16–25. https://doi.org/10.1016/j.ijantimicag.2017.11.002
27. Hoppe P-A, Holzhauer S, Lala B, Bührer C, Gratopp A, Hanitsch LG, Humme D, Kieslich M, Kallinich T, Lau S, *et al.* Severe infections of Panton-Valentine leukocidin positive Staphylococcus aureus in children. *Medicine (Baltimore)*. 2019:98:e17185. https://doi.org/10.1097/MD.0000000000017185
28. Rimoldi SG, Pileri P, Mazzocco MI, Romeri F, Bestetti G, Calvagna N, Tonielli C, Fiori L, Gigantiello A, Pagani C, *et al.* The role of Staphylococcus aureus in mastitis: a multidisciplinary working group experience. *J Hum Lact*. 2020:36:503–509. https://doi.org/10.1177/0890334419876272
29. Le Thomas I, Mariani-Kurkdjian P, Collignon A, Gravet A, Clermont O, Brahimi N, Gaudelus J, Aujard Y, Navarro J, Beaufils F, *et al.* Breast milk transmission of a Panton-Valentine leukocidin-producing Staphylococcus aureus strain causing infantile pneumonia. *J Clin Microbiol*. 2001:39:728–729. https://doi.org/10.1128/JCM.39.2.728-729.2001
30. Labandeira-Rey M, Couzon F, Boisset S, Brown EL, Bes M, Benito Y, Barbu EM, Vazquez V, Höök M, Etienne J, *et al.* Staphylococcus aureus Panton-Valentine leukocidin causes necrotizing pneumonia. *Science*. 2007:315:1130–1133. https://doi.org/10.1126/science.1137165
31. Gillet Y, Issartel B, Vanhems P, Lina G, Vandenesch F, Etienne J, Floret D, *et al.* Severe staphylococcal pneumonia in children. *Arch Pédiatrie*. 2001:8:742s–746s. https://doi.org/10.1016/S0929-693X(01)80190-1
32. Li HT, Zhang TT, Huang J, Zhou YQ, Zhu JX, Wu BQ. Factors associated with the outcome of life-threatening necrotizing pneumonia due to community-acquired Staphylococcus aureus in adult and adolescent patients. *Respiration*. 2011:81:448–460. https://doi.org/10.1159/000319557
33. Duployez C, Le Guern R, Tinez C, Lejeune A-L, Robriquet L, Six S, Loïez C, Wallet F, *et al.* Panton-valentine leukocidin secreting staphylococcus aureus pneumonia complicating COVID-19. *Emerg Infect Dis*. 2020:26:1939–1941. https://doi.org/10.3201/eid2608.201413
34. Nygaard U, Petersen A, Larsen AR, Rytter MJH, Hartling U, Kirkby N, Hansen RN, Nielsen AB, Lundstrøm K, Holm M, *et al.* Fatal SARS-CoV-2-associated panton-valentine Leukocidin-producing staphylococcal bacteremia: a nationwide multicenter cohort study. *Pediatr Infect Dis J*. 2022:41:e142–e145. https://doi.org/10.1097/INF.0000000000003476
35. Allou N, Allyn J, Traversier N, Baron M, Blondé R, Dupieux C, Coolen-Allou N, Jabot J, Miltgen G, *et al.* SARS-CoV-2 with Panton-Valentine leukocidin-producing Staphylococcus aureus healthcare-associated pneumonia in the Indian Ocean. *Heliyon*. 2022:8:e10422. https://doi.org/10.1016/j.heliyon.2022.e10422
36. Schaumburg F, Witten A, Flamen A, Stoll M, Alabi AS, Kremsner PG, Löffler B, Zipfel PF, Velavan TP, Peters G, *et al.* Complement 5a receptor polymorphisms are associated with panton-valentine leukocidin–positive Staphylococcus aureus colonization in African pygmies. *Clin Infect Dis*. 2019:68:854–856. https://doi.org/10.1093/cid/ciy666
37. Tromp AT, Van Gent M, Abrial P, Martin A, Jansen JP, De Haas CJC, Van Kessel KPM, Bardoel BW, Kruse E, Bourdonnay E, *et al.* Human CD45 is an f-component-specific receptor for the staphylococcal toxin Panton-Valentine leukocidin. *Nat Microbiol*. 2018:3:708–717. https://doi.org/10.1038/s41564-018-0159-x
38. Spaan A, Henry T, van Rooijen WM, Perret M, Badiou C, Aerts P, Kemmink J, de Haas CC, van Kessel KM, Vandenesch F, *et al.* The staphylococcal toxin panton-valentine leukocidin targets human C5a receptors. *Cell Host Microbe*. 2013:13:584–594. https://doi.org/10.1016/j.chom.2013.04.006
39. Alonzo F, Torres VJ. Bacterial survival amidst an immune onslaught: the contribution of the Staphylococcus aureus Leukotoxins. *PLoS Pathog*. 2013:9:e1003143. https://doi.org/10.1371/journal.ppat.1003143
40. Spaan AN, Van Strijp JAG, Torres VJ. Leukocidins: staphylococcal bi-component pore-forming toxins find their receptors. *Nat Rev Microbiol*. 2017:15:435–447. https://doi.org/10.1038/nrmicro.2017.27

Downloaded from https://academic.oup.com/jleukbio/article/115/2/222/7379048 by MPI Infection Biology user on 22 April 2024

41. Holzinger D, Gieldon L, Mysore V, Nippe N, Taxman DJ, Duncan JA, Broglie PM, Marketon K, Austermann J, Vogl T, *et al.* Staphylococcus aureus Panton-Valentine leukocidin induces an inflammatory response in human phagocytes via the NLRP3 inflammasome. *J Leukoc Biol*. 2012:92(5):1069–1081. https://doi.org/10.1189/jlb.0112014
42. van Kessel KPM, Bestebroer J, van Strijp JAG. Neutrophil-Mediated Phagocytosis of Staphylococcus aureus. *Front Immunol*. 2014:5:467. https://doi.org/10.3389/fimmu.2014.00467
43. Buvelot H, Posfay-Barbe KM, Linder P, Schrenzel J, Krause KH. Staphylococcus aureus, phagocyte NADPH oxidase and chronic granulomatous disease. *FEMS Microbiol Rev*. 2017:41:139–157. https://doi.org/10.1093/femsre/fuw042
44. Brinkmann V, Reichard U, Goosmann C, Fauler B, Uhlemann Y, Weiss DS, Weinrauch Y, Zychlinsky A, *et al.* Neutrophil extracellular traps kill bacteria. *Science*. 2004:303:1532–1535. https://doi.org/10.1126/science.1092385
45. Kenny EF, Herzig A, Krüger R, Muth A, Mondal S, Thompson PR, Brinkmann V, Bernuth Hv, Zychlinsky A, *et al.* Diverse stimuli engage different neutrophil extracellular trap pathways. *Elife*. 2017:6:e24437. https://doi.org/10.7554/eLife.24437
46. Fuchs TA, Abed U, Goosmann C, Hurwitz R, Schulze I, Wahn V, Weinrauch Y, Brinkmann V, Zychlinsky A, *et al.* Novel cell death program leads to neutrophil extracellular traps. *J Cell Biol*. 2007:176:231–241. https://doi.org/10.1083/jcb.200606027
47. Papayannopoulos V, Metzler KD, Hakkim A, Zychlinsky A. Neutrophil elastase and myeloperoxidase regulate the formation of neutrophil extracellular traps. *J Cell Biol*. 2010:191:677–691. https://doi.org/10.1083/jcb.201006052
48. Sollberger G, Choidas A, Burn GL, Habenberger P, Di Lucrezia R, Kordes S, Menninger S, Eickhoff J, Nussbaumer P, Klebl B, *et al.* Gasdermin D plays a vital role in the generation of neutrophil extracellular traps. *Sci Immunol*. 2018:3:eaar6689. https://doi.org/10.1126/sciimmunol.aar6689
49. Pilsczek FH, Salina D, Poon KKH, Fahey C, Yipp BG, Sibley CD, Robbins SM, Green FHY, Surette MG, Sugai M, *et al.* A novel mechanism of rapid nuclear neutrophil extracellular trap formation in response to Staphylococcus aureus. *J Immunol*. 2010:185:7413–7425. https://doi.org/10.4049/jimmunol.1000675
50. Bhattacharya M, Berends ETM, Chan R, Schwab E, Roy S, Sen CK, Torres VJ, Wozniak DJ, *et al.* Staphylococcus aureus biofilms release leukocidins to elicit extracellular trap formation and evade neutrophil-mediated killing. *Proc Natl Acad Sci U S A*. 2018:115:7416–7421. https://doi.org/10.1073/pnas.1721949115
51. Mazzoleni V, Zimmermann-Meisse G, Smirnova A, Tarassov I, Prévost G. Staphylococcus aureus Panton-Valentine Leukocidin triggers an alternative NETosis process targeting mitochondria. *FASEB J*. 2021:35:e21167. https://doi.org/10.1096/fj.201902981R
52. Berends ETM, Horswill AR, Haste NM, Monestier M, Nizet V, Von Köckritz-Blickwede M. Nuclease expression by Staphylococcus aureus facilitates escape from neutrophil extracellular traps. *J Innate Immun*. 2010:2:576–586. https://doi.org/10.1159/000319909
53. Heyworth PG, Cross AR, Curnutte JT. Chronic granulomatous disease. *Curr Opin Immunol*. 2003:15:578–584. https://doi.org/10.1016/s0952-7915(03)00109-2
54. Losman MJ, Fasy TM, Novick KE, Monestier M. Monoclonal autoantibodies to subnucleosomes from a MRL/Mp(-)+/+ mouse. Oligoclonality of the antibody response and recognition of a determinant composed of histones H2A, H2B, and DNA. *J Immunol*. 1992:148:1561–1569. https://doi.org/10.4049/jimmunol.148.5.1561
55. Hughes CS, Moggridge S, Müller T, Sorensen PH, Morin GB, Krijgsveld J. Single-pot, solid-phase-enhanced sample preparation for proteomics experiments. *Nat Protoc*. 2019:14:68–85. https://doi.org/10.1038/s41596-018-0082-x
56. Plubell DL, Wilmarth PA, Zhao Y, Fenton AM, Minnier J, Reddy AP, Klimek J, Yang X, David LL, Pamir N, *et al.* Extended multiplexing of tandem mass tags (TMT) labeling reveals age and high fat diet specific proteome changes in mouse epididymal adipose tissue. *Mol Cell Proteomics*. 2017:16:873–890. https://doi.org/10.1074/mcp.M116.065524
57. Robinson MD, McCarthy DJ, Smyth GK. Edger: a Bioconductor package for differential expression analysis of digital gene expression data. *Bioinformatics*. 2010:26:139–140. https://doi.org/10.1093/BIOINFORMATICS/BTP616
58. Ritchie ME, Phipson B, Wu D, Hu Y, Law CW, Shi W, Smyth GK, *et al.* Limma powers differential expression analyses for RNA-sequencing and microarray studies. *Nucleic Acids Res*. 2015:43:e47. https://doi.org/10.1093/nar/gkv007
59. Kammers K, Cole RN, Tiengwe C, Ruczinski I. Detecting significant changes in protein abundance. *EuPA Open Proteom*. 2015:7:11–19. https://doi.org/10.1016/j.euprot.2015.02.002
60. Larsson J. eulerr: Area-Proportional Euler and Venn Diagrams with Ellipses. R package version 6.1.1. 2021. Available: https://cran.r-project.org/package = eulerr
61. Kolde R. pheatmap: Pretty Heatmaps. R package version 1.0.12. 2019.
62. Perez-Riverol Y, Csordas A, Bai J, Bernal-Llinares M, Hewapathirana S, Kundu DJ, Inuganti A, Griss J, Mayer G, Eisenacher M, *et al.* The PRIDE database and related tools and resources in 2019: improving support for quantification data. *Nucleic Acids Res*. 2019:47:D442–D450. https://doi.org/10.1093/nar/gky1106
63. Amulic B, Knackstedt SL, Abu Abed U, Deigendesch N, Harbort CJ, Caffrey BE, Brinkmann V, Heppner FL, Hinds PW, Zychlinsky A, *et al.* Cell-Cycle proteins control production of neutrophil extracellular traps. *Dev Cell*. 2017:43:449–462.e5. https://doi.org/10.1016/j.devcel.2017.10.013
64. Sanders SA, Eisenthal R, Harrison R. NADH Oxidase activity of human xanthine oxidoreductase generation of superoxide anion. *Eur J Biochem*. 1997:245:541–548. https://doi.org/10.1111/j.1432-1033.1997.00541.x
65. Li Y, Trush MA. Diphenyleneiodonium, an NAD(P)H oxidase inhibitor, also potently inhibits mitochondrial reactive oxygen species production. *Biochem Biophys Res Commun*. 1998:253:295–299. https://doi.org/10.1006/bbrc.1998.9729
66. Majander A, Finel M, Wikström M. Diphenyleneiodonium inhibits reduction of iron-sulfur clusters in the mitochondrial NADH-ubiquinone oxidoreductase (Complex I). *J Biol Chem*. 1994:269:21037–21042. https://doi.org/10.1016/s0021-9258(17)31926-9
67. Galbusera C, Orth P, Fedida D, Spector T. Superoxide radical production by allopurinol and xanthine oxidase. *Biochem Pharmacol*. 2006:71:1747–1752. https://doi.org/10.1016/j.bcp.2006.02.008
68. Metzler KD, Goosmann C, Lubojemska A, Zychlinsky A, Papayannopoulos V. Myeloperoxidase-containing complex regulates neutrophil elastase release and actin dynamics during NETosis. *Cell Rep*. 2014:8:883–896. https://doi.org/10.1016/j.celrep.2014.06.044
69. Petretto A, Bruschi M, Pratesi F, Croia C, Candiano G, Ghiggeri G, Migliorini P. Neutrophil extracellular traps (NET) induced by different stimuli: A comparative proteomic analysis. *PLoS One*. 2019:14:1–18. https://doi.org/10.1371/journal.pone.0218946

Downloaded from https://academic.oup.com/jleukbio/article/115/2/222/7379048 by MPI Infection Biology user on 22 April 2024

70. Scola AM, Johswich KO, Morgan BP, Klos A, Monk PN. The human complement fragment receptor, C5L2, is a recycling decoy receptor. *Mol Immunol*. 2009:46:1149–1162. https://doi.org/10.1016/j.molimm.2008.11.001
71. Bamberg CE, Mackay CR, Lee H, Zahra D, Jackson J, Lim YS, Whitfeld PL, Craig S, Corsini E, Lu B, *et al.* The C5a receptor (C5aR) C5L2 is a modulator of C5aR-mediated signal transduction. *J Biol Chem*. 2010:285:7633–7644. https://doi.org/10.1074/jbc.M109.092106
72. Genestier A-L, Michallet M-C, Prévost G, Bellot G, Chalabreysse L, Peyrol S, Thivolet F, Etienne J, Lina G, Vallette FM, *et al.* Staphylococcus aureus Panton-Valentine leukocidin directly targets mitochondria and induces Bax-independent apoptosis of human neutrophils. *J Clin Invest*. 2005:115:3117–3127. https://doi.org/10.1172/JCI22684
73. Badiou C, Dumitrescu O, George N, Forbes ARN, Drougka E, Chan KS, Ramdani-Bouguessa N, Meugnier H, Bes M, Vandenesch F, *et al.* Rapid detection of Staphylococcus aureus Panton-Valentine Leukocidin in clinical specimens by enzyme-linked immunosorbent assay and immunochromatographic tests. *J Clin Microbiol*. 2010:48:1384–1390. https://doi.org/10.1128/JCM.02274-09
74. Malachowa N, Kobayashi SD, Freedman B, Dorward DW, DeLeo FR. Staphylococcus aureus leukotoxin GH promotes formation of neutrophil extracellular traps. *J Immunol*. 2013:191:6022–6029. https://doi.org/10.4049/jimmunol.1301821
75. Grosz M, Kolter J, Paprotka K, Winkler A-C, Schäfer D, Chatterjee SS, Geiger T, Wolz C, Ohlsen K, Otto M, *et al.* Cytoplasmic replication of Staphylococcus aureus upon phagosomal escape triggered by phenol-soluble modulin α. *Cell Microbiol*. 2014:16:451–465. https://doi.org/10.1111/cmi.12233
76. Fuchs TA, Brill A, Duerschmied D, Schatzberg D, Monestier M, Myers DD, Wrobleski SK, Wakefield TW, Hartwig JH, Wagner DD, *et al.* Extracellular DNA traps promote thrombosis. *Proc Natl Acad Sci U S A*. 2010:107:15880–15885. https://doi.org/10.1073/pnas.1005743107
77. Kahlenberg JM, Carmona-Rivera C, Smith CK, Kaplan MJ. Neutrophil extracellular trap-associated protein activation of the NLRP3 inflammasome is enhanced in lupus macrophages. *J Immunol*. 2013:190:1217–1226. https://doi.org/10.4049/jimmunol.1202388
78. Apel F, Andreeva L, Knackstedt LS, Streeck R, Frese CK, Goosmann C, Hopfner K-P, Zychlinsky A, *et al.* The cytosolic DNA sensor cGAS recognizes neutrophil extracellular traps. *Sci Signal*. 2021:14:eaax7942. https://doi.org/10.1126/scisignal.aax7942

Downloaded from https://academic.oup.com/jleukbio/article/115/2/222/7379048 by MPI Infection Biology user on 22 April 2024